

ARTICLE OPEN



Uncertainties in measuring precipitation hinders precise evaluation of loss of diversity in biomes and ecotones

Andrés Navarro¹✉, Gyuwon Lee², Raúl Martín³ and Francisco J. Tapiador¹

Assessing changes in the distribution of biological communities that share a climate (biomes) is essential for estimating their vulnerability to climate change. We use CMIP6 climate models to calculate biome changes as featuring in classifications such as Holdridge's Life Zones (climate envelopes). We found that transitional zones between biomes (known as ecotones) are expected to decline under all climate change scenarios, but also that model consensus remains low. Accurate assessments of diversity loss are limited to certain areas of the globe, while model consensus is still poor for half of the planet. We identify where there are robust estimates of changes in biomes and ecotones, and where consensus is lacking. We argue that caution should be exercised in measuring biodiversity loss in the latter, but that greater confidence can be placed in the former. We find that shortcomings in the life zone classification are related to inter-model variability, which ultimately depends on a larger problem, namely the accurate estimation of precipitation compared to CRU. Application of the methodology to other climate classifications confirms the findings.

npj Climate and Atmospheric Science (2024)7:35; <https://doi.org/10.1038/s41612-024-00581-w>

INTRODUCTION

Biomes are biological communities sharing a climate. Ecotones are their transition zones. It is accepted that anthropogenic climate change has already generated an impact on the global distribution of biomes, causing disruptions in the ecological functions and loss of biodiversity. That has resulted in more vulnerable environments^{1–3}. Changes in ecotones have been more severe as these regions are not simple transient zones but have unique ecological characteristics defined by the interaction of neighboring biomes^{4–6}. A particular combination of habitats tends to create new ecological niches and that has increased biodiversity through evolution.

Biomes and ecotones are also considered areas of primary interest for climate change studies. They are especially sensitive to fluctuations, thus acting as an early warning about impacts of anthropogenic climate change^{7–9}. The process can be explained in purely mechanistic terms since biomes and ecotones account for the fluxes of matter and energy that affect the biota (e.g., through nutrient cycling). The impact of climate change is particularly acute in ecotones, where species are pushed to their limits in a context of unstable equilibrium⁵.

The climate is the main factor that shapes the distribution of biomes¹⁰. Soil, latitude, anthropic pressure and existing flora are secondary factors^{11–13}. There is agreement in that biomes can be characterized by a few abiotic factors such as temperature and rainfall^{14–16} and that these ecological units are a robust dimensional reduction for complex plant-specific physiological thresholds of heat and water demand^{17–19}. In particular, Holdridge's scheme (HLZ) provides a comprehensive classification system to describe both life zones and ecotones from those environmental factors. The latter feature is not present in the original formulation of the method but an enhancement through a minor adaptation^{20,21} (Fig. 1a).

Biome classification using Holdridge's system, can be carried out through climate model outputs. Current Earth System Models

(ESMs) have evolved beyond Global Climate Models (GCMs) and now include the main physical and biogeochemical processes of the Earth²². Such enhancements build confidence in these models having a superior ability to account for biological factors, and in particular the distribution of life on Earth. The combination of ESM climate outputs with classifications such as the HLZ scheme define climate envelopments in an objective way.

The ability of any method to characterize biomes and ecotones can be evaluated by comparing a present-climate classification from ESM outputs with an actual classification using measurements (ground observations or satellite data). This is a necessary (but no sufficient) condition to gauge ESM capabilities, and also a means to identify those areas where most models agree and where models strongly disagree. But perhaps more importantly, such validation helps identify potential shortcomings in the modeling, thus informing on the limitations and uncertainties in the predicted changes in biomes and ecotones. Indeed, guidance on the error source is also beneficial not only for climate modelers but also for life scientists, who make use of model output for their own research interests. Thus, a comprehensive understanding of errors helps to develop a more meaningful analysis of the consequences of climate change²³.

RESULTS

Biome distribution in present climate

We first assess how well Coupled Model Intercomparison Project phase 6 (CMIP6) models characterize current biomes. Thus we compared the model-derived classification with the observations from the Climate Research Unit (CRU) Time Series (TS) dataset (CRU, Fig. 1b). For the present climate, an overall moderate consensus appears ($0.4 \leq \kappa \leq 0.7$). Regarding precipitation, we found that a good performance in the representation of the field ($R^2 \geq 0.7$) is essential to obtain acceptable kappa coefficients, although there are exceptions, namely CESM2, MIROC6 and

¹Earth and Space Sciences (ESS) Group, Institute of Environmental Sciences (ICAM), University of Castilla-La Mancha (UCLM), Avda. Carlos III s/n, 45071 Toledo, Spain. ²Department of Atmospheric Sciences, Center for Atmospheric REmote sensing (CARE), Kyungpook National University, Daegu, Republic of Korea. ³Department of Mathematics, University of Castilla-La Mancha (UCLM), Avda. Carlos III s/n, 45071 Toledo, Spain. ✉email: Andres.Navarro@uclm.es

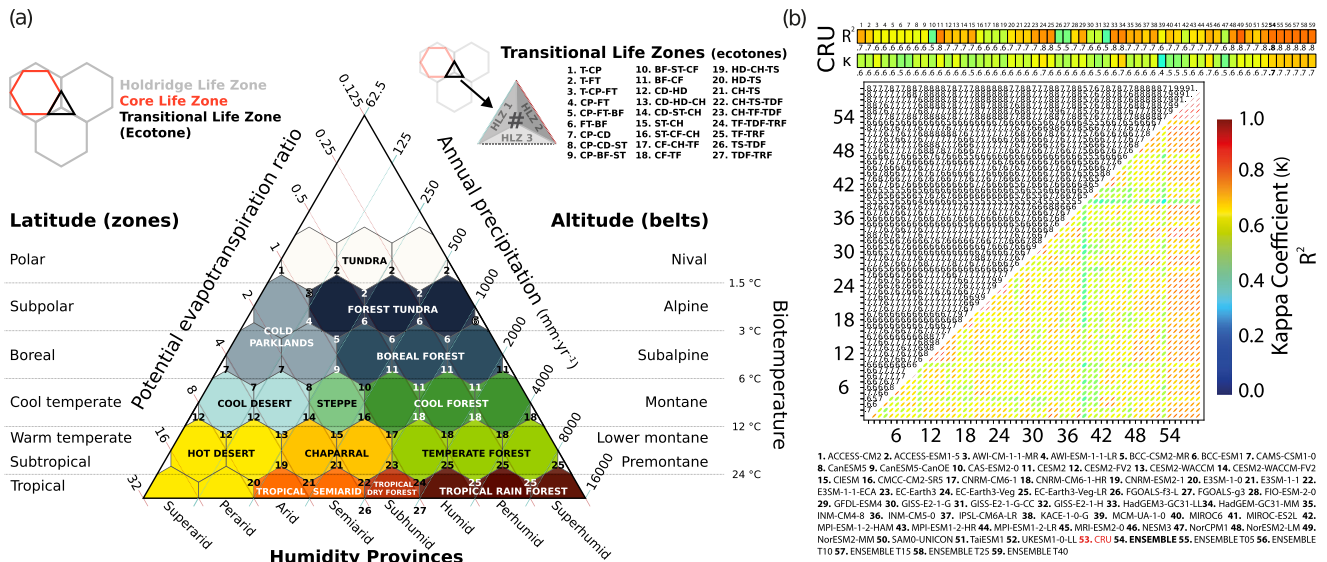


Fig. 1 Holdridge life zones classification scheme and class agreement for CMIP6 models and reference dataset. **a** The HLZ system shows the location of each life zone according to biotemperature, potential evapotranspiration ratio, and annual precipitation; the original 38 zones were aggregated into 13 core zones and 27 ecotones (TLZs) following Monserud & Leeman⁸⁰. **b** Class agreement chart, the upper-left triangle shows the Kappa coefficient matrix (k ; 1 perfect agreement; 0 no agreement) and the bottom-right displays the correlation ellipsoids between classes. The bars on the top of the figure are k and R^2 coefficients of each model when compared with reference dataset (CRU).

CIESM. In these, good scores for precipitation estimates are not translated into better representation of HLZs. Only three models—HadGEM-GC31-MM, EC-Earth-Veg and UKESM1-0-LL—achieved the best scores in both R^2 and kappa, but the six ensembles do agree. Models reproduce the spatial distribution of major biomes (Fig. 2a–c) but discrepancies are indeed found around the limits of life zones where large inter-model variability is observed, i.e., the ecotones (see supplementary material for a panel plot of individual models, Supplementary Fig. 1).

Dissent is found in areas with complex orography such as the Rocky Mountains, the Andes, and the Himalayas. There, models have difficulties in reproducing the heterogeneous distribution of biomes. The ‘Cold Parklands’ category is misclassified in most models confirming the limitation ESMS have to classify climate types when extreme values are involved²⁴. Almost no model can properly characterize the extremely humid tropical rainforest in the Amazonia and the same for the extremely hot desert in central Australia.

Most of the model-observations biases are found in regions with moderate-to-large inter-model variability, as depicted by Fig. 2d (stripes). The lack of consensus over these areas means that some key processes are not well modeled yet. We point below to those related to the water cycle modeling, Fig. 2e, f (See Table 1 for a description of the methods).

In spite of biases, consensus between the top-10 models and the reference data is above 51% of the total area ($\geq 80\%$ models agree). The consensus area covers a wide range of habitats; including hot deserts, such as the Sahara and the Arabian deserts, rainforests of South-east Asia, and cool and temperate forests of western Europe and eastern US.

Ecotones in present climate

As transition areas, ecotones are more challenging than biomes. A precise characterization of ecotones for the present climate is however essential to use model outputs as a guide for future climate shifts, especially when the projected changes are expected to be more pronounced in transitional areas^{25–27}.

We compared the models with CRU data and found that the individual models identify the major ecotones. However, they cannot capture the transition zones of some of them, such as Cold

Parklands (TLZs 3,4,5,7 and 8). The problem could be identified in the CP-FT-BF (TLZ 5) where the ecotone is absent in most models (see Supplementary Fig. 3 for individual models). This is a consequence of wet bias that is amplified by the log-scaling, where minor changes in the lower bounds produce large impacts. The southward displacement of the TLZs 21 and 23 is another important error source, as illustrated in Fig. 2(g, h). This pattern is observed in southern Africa where the wet bias causes the misrepresentation of the transition between tropical dry forest, savanna, and the Afromontane forest.

Regarding the dry bias over land, this is a known shortcoming of models^{28–30}. The causes are a matter of discussion^{31–33} but the feature is not controversial and is accounted for when model data are used in the biological realm^{34,35}. Here, we found that the dry bias features in the HLZ classification in several places, such as an increase in the eastward expansion of tropical semi-arid-tropical dry ecotone in India (TLZ 22).

We have found that models overestimate the global extension of ecotones by 2%. The main cause is the artificial expansion of the transitional zone of tropical rainforest and tropical dry forest (TLZ 24). An example of this process can be seen in the Amazonia. In that region, the ensemble mean underestimates annual precipitation, causing a dry bias that expands the tropical rain-dry ecotone. The effect is palliated in the top-10 ensemble (a subset of the ensemble) thanks to their better estimation of precipitation, as shown in Supplementary Fig. 5.

Indeed, models with better precipitation estimates produce more credible biomes and ecotones. Model ensembles benefit greatly from these good models but cannot completely compensate those with unrealistic precipitation estimates. Overall, the multi-model ensemble (MME, 52 members) correctly features the continuous bands of forest tundra-taiga transition (TLZ 6) as well as steppe-cool forest-boreal forest ecotones (TLZs 16 and 11) but barely captures the extension and the precise location of these TLZs. The MME estimates colder temperatures in northern Eurasia and shifts TLZ 6 and TLZ 11 to the south while the wet bias increases the forest-steppe ecotone in central US (TLZ 16). The top-10 ensemble reduces some of those biases but location problems remain, meaning that the problem is shared by most models. This is more clearly seen in the accuracy in rainfall

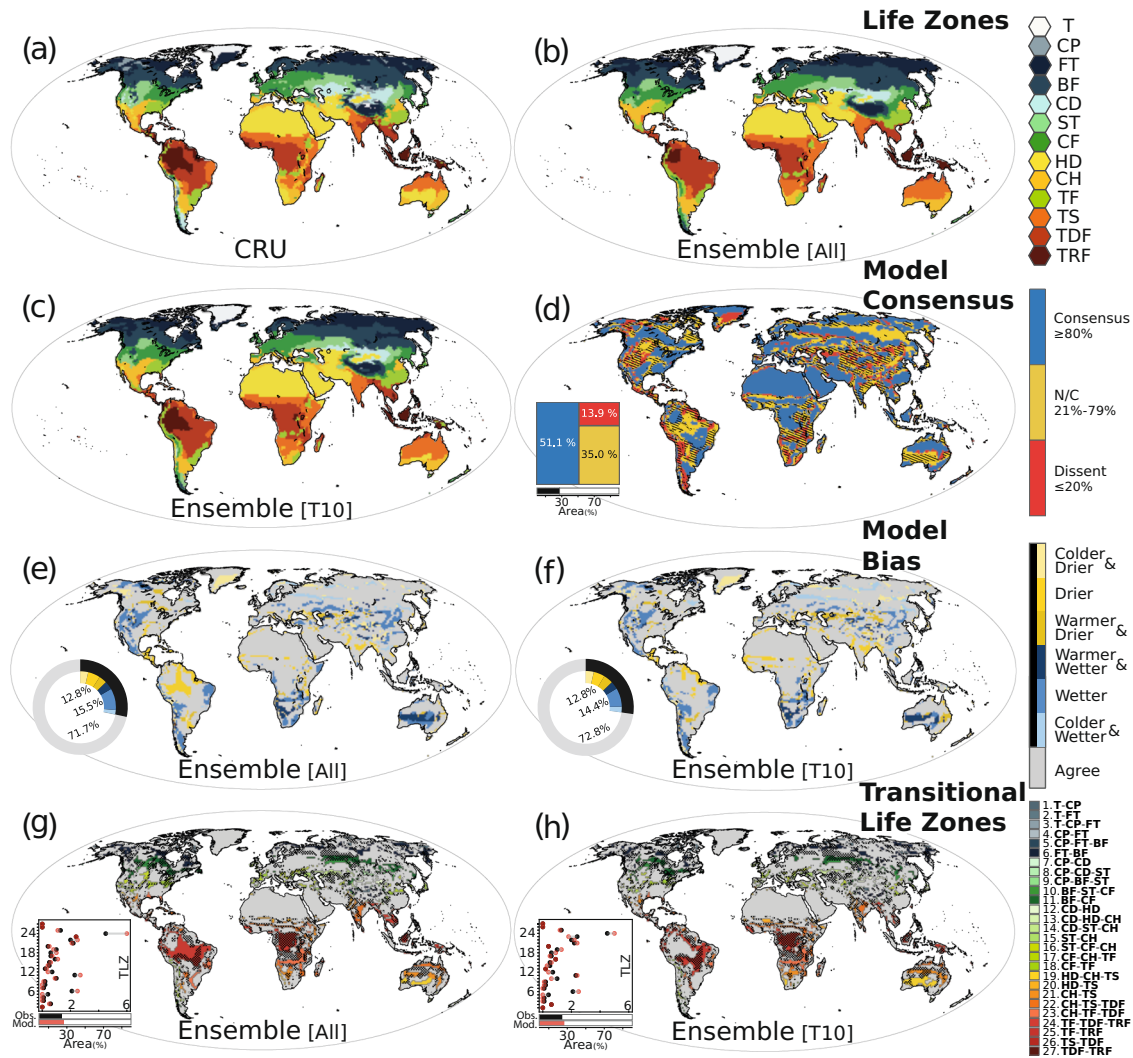


Fig. 2 Global distribution of life zones, ecotones, and consensus map for present climate (1980–2014). Global maps of life zones for CRU dataset (a), multi-model ensemble mean of fifty-two members (b), and ensemble mean of top ten rated climate models (c). d Consensus map of life zones based on top ten CMIP6 models (T10). Blues are regions where most models agree with reference dataset ($\geq 80\%$), yellows are regions with moderate consensus (21–79%), and reds are regions with low consensus ($\leq 20\%$). Stripes are regions with large inter-model variability (half of the fifty-two models disagree in the type of life zone). The treemap shows the percentage of the area covered by each category. The barplot shows the percentage of the total area with large inter-model variability. e, f Deconstruction of errors in the multi-model ensemble mean and T10 ensemble mean. Yellow, light yellow and dark yellow are drier, colder and drier, and warmer & drier conditions than reference data. Blue, dark blue and light blue are wetter, warmer and wetter, and colder and wetter conditions. The agreement between modeled and observed life zones is colored in gray (100% agreement). Double donut plots distribute the proportion of global agreement/disagreement. g, h Global distribution maps of ecotones for multi-model ensemble mean (g) and T10 ensemble mean (h). The stippling shows the distribution of ecotones as depicted by CRU. Inset steam plots compare observed (black) and modeled (red) area that is covered by each one of the twenty-seven ecotones (TLZs). Bar plots show the percentage of the total area covered by ecotones.

estimates in the Maritime Continent, which yields a better characterization of the temperate and rain forests ecotone (TLZ 25). This contrasts to the wet bias observed in central Australia which harms the representation of transitional areas between hot desert, tropical semiarid and the Kwongan, a chaparral-like ecoregion (TLZs 19 and 21).

Deconstructing biases

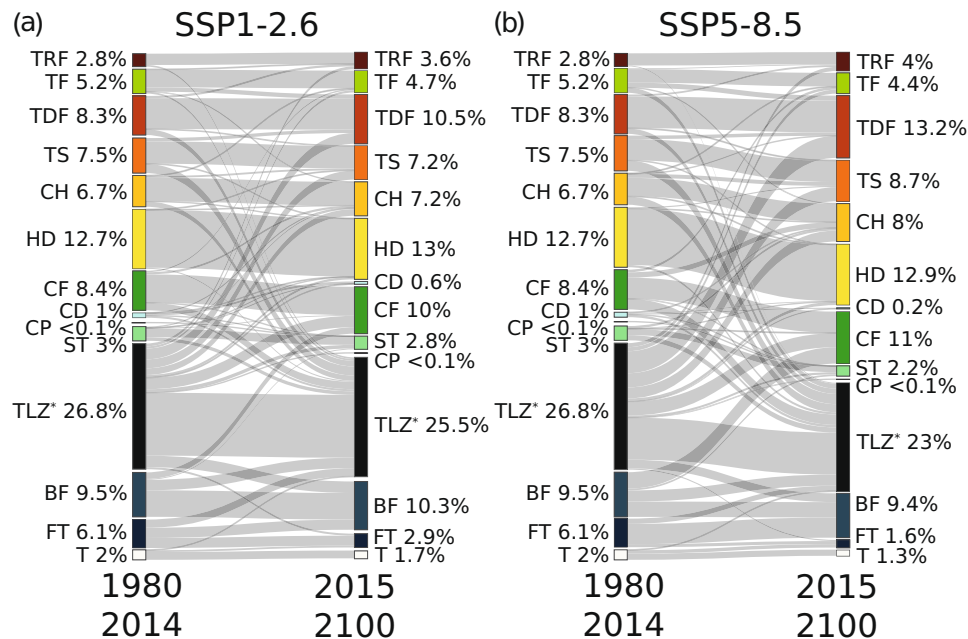
Because Holdridge's classes are calculated from monthly climatologies of temperature and precipitation, we can decompose the specific biases that are responsible for errors in the representation of biomes and ecotones (Fig. 2e, f). We found that both ensembles have similar results, but the top-10 ensemble obtains slightly

better scores thanks to bias reduction in the Amazonia and central Australia. The advantage is only apparent because an ensemble with few members minimizes the inter-model variability, a crucial problem in those regions^{36–38}. Moreover, the top-10 ensemble intensifies the bias in key transient zones for future climate, such as steppe-cool forest (TLZ 10) and temperate forest-tropical dry forest ecotones (TLZ 23).

As argued above, most of the error can be explained by deficiencies in modeled rainfall. One exception is the southward propagation of boreal forest over Eurasia where models predict colder conditions than reference data (see Supplementary Fig. 2 for individual maps of model bias and Supplementary Fig. 4 for MAB). Precipitation plays the main role in the dry bias observed in the Caribbean, which is a common feature in all models^{39,40}. Wet

Table 1. Criteria for deconstructing model errors in Holdridge's Life Zones scheme.

Model bias	Annual precipitation	Biotope temperature	PET ratio	Cause
Colder-drier	Obs > Mod	Obs > Mod	Obs ≥ Mod	Temp. & Prec.
Drier	Obs > Mod	Obs = Mod	Obs < Mod	Precipitation
Warmer-drier	Obs = Mod	Obs < Mod	Obs < Mod	Temperature
Warmer-wetter	Obs < Mod	Obs < Mod	Obs ≤ Mod	Prec. & Temp.
Wetter	Obs < Mod	Obs = Mod	Obs > Mod	Precipitation
Colder-wetter	Obs = Mod	Obs > Mod	Obs > Mod	Temperature

**Fig. 3** Life zone area changes from present climate (1980–2014) to future climate (2015–2100). Flow diagrams for the low-emission scenario SSP1-2.6 (a) and high-emission scenario SSP5-8.5 (b). The twenty-seven ecotones were aggregated into one category (TLZ*) for a better visualization.

bias in west US is also a shared problem caused by a misrepresentation of the precipitation field⁴¹. Modeling the seasonal displacement of the Intertropical Convergence Zone (ITCZ) is yet another problem. It results in a wet bias in northeastern Brazil and southern Africa in boreal winter and in the East Asian summer monsoon^{42,43}.

Sources of error in modeled precipitation can be attributable to microphysics, convection, boundary layer and radiation parameterizations. The coarse resolution of CMIP6 models is also important for small-scale precipitation, which is usually parameterized. Models have also known problems to simulate the orographic effects over major mountain chains because the complex interactions between dynamics, thermodynamics, and microphysics⁴⁴. The problem is highlighted in areas near arid regions where minor changes in precipitation produce large differences between life zones.

Better precipitation estimates—not better temperature estimates, or more spatial resolution—translates into a better classification of biomes and ecotones in Holdridge system. However, it is worth noting that a good precipitation score does not directly translate to a more precise class in the biome or in the ecotone classification so the previous observation is not as obvious as it may seem. Classes in Holdridge system stem from a series of thresholds, cut-offs and intervals and there is not a univocal relationship between both ranks.

Future climate

Uncertainties are inherently greater in climate projections as these include scenarios that model economic and social behavior. The future unknowns involved are addressed in the community by introducing Shared Socio-Economic Pathways (SSPs)⁴⁵ or scenarios.

We used the seven standard SSPs in our calculations. Regarding ecotones, both the so-called optimistic and worst-case scenarios (see Supplementary Fig. 29 for other SSP) show the same pattern for the direction of the changes (Fig. 3a, b). Flow diagrams for these extreme cases depict an important reduction of tundra and forest tundra life zones, a global decrease in the extent of the ecotones, and an increase of warm and tropical life zones. The major difference between scenarios is found in the intensity of these changes. Thus, for example, the MME predicts a much more intense decline of TLZs in SSP5-8.5 (3.8% of total area) than in SSP1-2.6 (1.3%).

The spatial representation of the flows (Fig. 4a, b) provides further insight into what could be expected in future climates. Thus, the severe reduction of subtropical forests (TF) in Africa clearly features in maps but is hidden in the flow diagrams due to the small change over total area and non-directional character of the flux diagrams. Maps also highlight the depletion of forest tundra in the Tibetan Plateau as well as the poleward expansion of

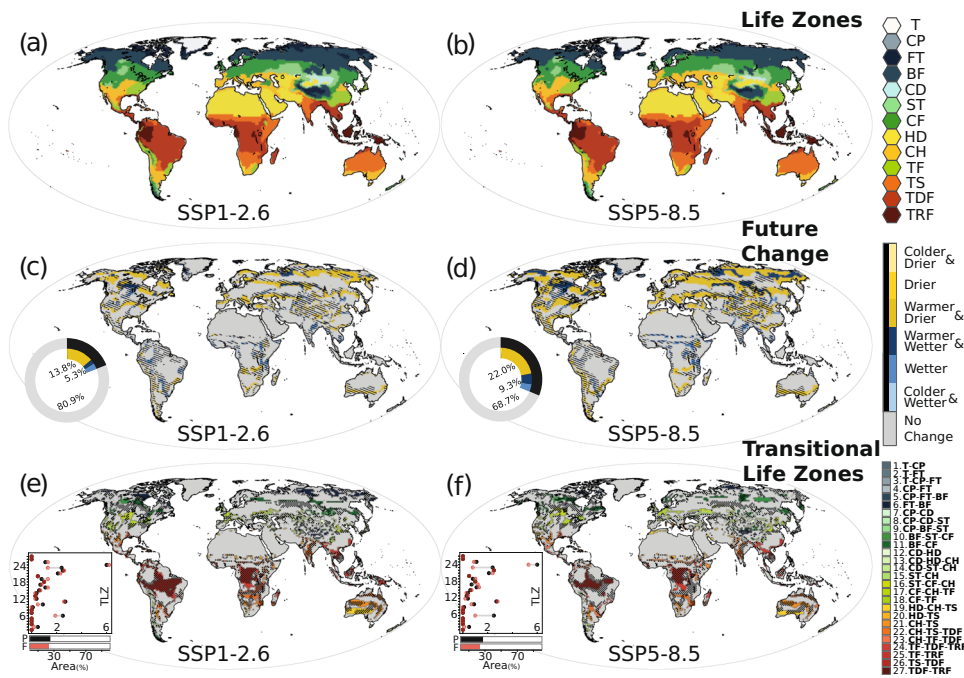


Fig. 4 Changes in the distribution of life zones and ecotones under two future climate scenarios. Global distribution of future life zones for SSP1-2.6 (a) and SSP5-8.5 (b) scenarios. c, d maps showing the direction of the changes in HLZ for the low-emission (c) and high-emission (d) scenarios. Yellows are shifts to drier zones (yellow: drier; light yellow: colder & drier; dark yellow: warmer & drier), blues are shifts to wetter zones (blue: wetter; light blue: colder & wetter; dark blue: warmer & wetter), and grays stand no changes. Stripes are regions with large inter-model variability. Double donut plots illustrate the proportion of each change type. e, f are maps of the distribution of ecotones under SSP1-2.6 (e) and SSP5-8.5 (f) scenarios. The stippling shows the distribution of ecotones for present climate. Inset stem plots show the change in the area covered by each TLZ. Bar plots are the percentage of the total area covered by TLZs for present (black) and future scenarios (red). The size of the ensemble is $n = 36$ for SSP1-2.6 and $n = 37$ for SSP5-8.5.

dry climates. The northward propagation of the chaparral in Europe is another process that features in all the SSPs.

The spatial consistency of the estimates changes builds confidence in the modeling. Moreover, the maps of differences show consensus between scenarios in the identification and the location of future shifts. These changes, however, differ in their extent (Fig. 4c, d). Shifts toward warmer and drier life zones were the most frequent type of change (14%–22%) while unchanging life zones range from 81%–69%, according to each SSP. In these areas, the expected variations in temperature and precipitation do not exceed the critical threshold for biome shift.

The location and extent of changes in the ecotones depend on the scenario (Fig. 4e, f). In some cases, the projections are disparate. SSP1-2.6 and SSP5-8.5 give opposite results in the transition zone between temperate and tropical forests (TLZs 24 and 25). The disagreement between the simulated changes in both scenarios is most apparent in the Amazonia and in the Maritime Continent where SSP5-8.5 reduces the extension of TLZs 24–25 in favor of tropical dry and tropical rain life zones.

Like biome shifts, most differences between scenarios appears in terms of signal strength, not in the direction of the change. Thus, the contraction of tundra-forest tundra-boreal forest ecotones (TLZs 2 and 6) is observed in all SSPs but with different magnitudes. Other shared pattern is the conversion of transitional areas between chaparral, temperate forest and tropical dry forest (TLZ 17 and 23) into new Holdridge's life zones. Past TLZ 17 is now identified as chaparral while the ecotone lies further north (e.g., in the eastern US and southern Europe). The case of TLZ 23 in central and eastern Africa is paradigmatic: the transition from subtropical temperate forest to tropical dry forest in the Angolan Highlands and the Afromontane forests will be completed by 2100 and, consequently, the total area covered by the ecotone will be reduced more than 33%. TLZ 10 will also decrease, but the impact

will be higher in low-emission scenarios (SSP1-1.9 and SSP1-2.6). Future projections include the expansion of few transient zones, such as the thorn woodland and desert scrub ecotone (TLZ 19). The increase is better observed in the 'optimistic' scenarios, as with TLZ 10.

DISCUSSION

The extent and intensity of biome and ecotone shifts—defined here by changes in climatic variables—have a wide impact on several Earth's cycles. For example, the expected reduction of forest-based biomes (−4.5%, excluding tropical dry forest) and the expansion of grasslands-shrublands (+9.3%) are transformations that will certainly affect biogeophysical processes (through albedo and evapotranspiration)⁴⁶, biogeochemical cycles (through the nutrient cycling)⁴⁷, and biogeographical processes⁴⁸. Changes in albedo are a well-known example of how biome disruptions can have a global impact.

The reduction of forest tundra and its ecotone (TLZ 2) also modifies the albedo and increases the cooling effect of the surface, altering the global energy flux⁴⁹. Similarly, the conversion of transitional zones between cool and temperate forests (TLZ 17) into chaparral modifies soil properties, diminishing its carbon storage capacity and nutrients^{50,51}. Nutrient deficiencies such as nitrogen and phosphorous minimizes the chances of recovering the system to the initial state creating a feedback loop.

Another interesting example of how biome disruptions are widespread is found in Africa. The increase of temperature accelerates water stress that reduces transient areas between subtropical moist forest and tropical dry forest (TLZ 23) and promotes the replacement of tall, multi-stratal closed canopies by open canopies and woodlands of drought-tolerant species⁵². The consequences in terms of the carbon and the nitrogen cycles are

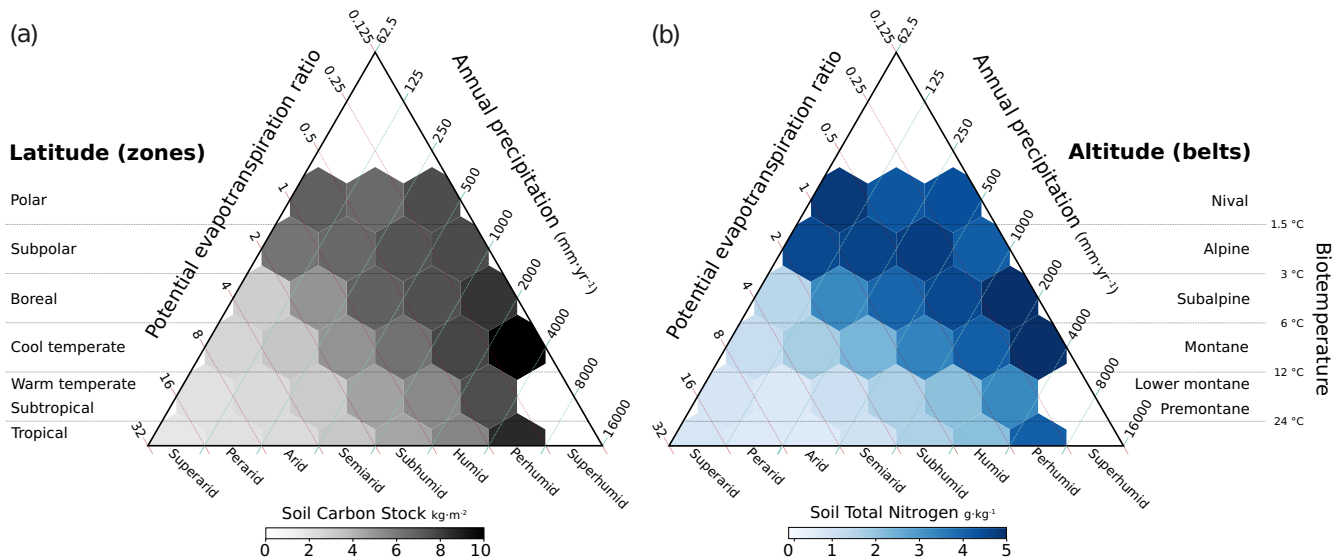


Fig. 5 Soil Carbon and Nitrogen by Holdridge Life Zones. Carbon Stock (a) and Total Nitrogen (b) of the topsoil (30 cm) in the Holdridge Life Zone scheme. Gridded data of carbon and nitrogen was obtained from the SoilGrids 2.0 dataset⁸⁰. Light (dark) colors indicate less (more) content of carbon/nitrogen in the topsoil.

well known^{53–55} (Fig. 5) and include lower carbon and nitrogen use efficiency, as well as less storage capacity.

In general, the transition to drier and warmer environments that we found reduces the ability of certain biomes to act as carbon sinks due to limited photosynthetic activity. As shown in Fig. 5, there is an inverse relationship between nutrient availability and the PET ratio (PET/precipitation), but the behavior of nitrogen is complex and more sensitive to small changes in temperature and precipitation, especially in colder environments (e.g. TLZ 6).

The cool deserts category is also affected by global warming. We expect a reduction that ranges from 40% to 80% of the total area according to each scenario. This biome shifts toward transitional zones between hot and cool deserts (TLZs 12 and 13) and, to a lesser degree, toward chaparral and hot desert life zones. It is obvious that increased temperatures enhance evaporation, accelerate soil water consumption, and reduce subsurface water storage, which intensifies dryness. But it is less obvious without making the actual calculations to which extent the new warmer and drier conditions increase the exposure to wildfires and favor biological invasions, compromising the survival of native species⁵⁶. The changes featured in the maps are consistent with a process in which the expansion of the desert decimates the biological communities at their fringes. Ecotones act then as a transient refuge for many species in harsh conditions. The system can go into non-recovery state if it is severely impacted.

Future changes also affect steppe (−26.6%) and cool forest (+23.6%) areas. For steppe, shifts are towards thorn steppe and dry forest ecotones (TLZs 14–16) and its neighboring life zones (chaparral and cool forest). Cool forest expands at the expense of boreal forest and the ecotones between deciduous forest, taiga, and steppe (TLZs 10 and 11). The consequences of these shifts are different although the major driver of change is the same: rising temperature. In the first case, shifts toward chaparral reinforce the main problems of moisture-limited biomes: soil degradation; water scarcity; and more pressure on resources. Those limitations are crucial for wildlife there, as species compete for pastures and freshwater. On the contrary, in temperature-limited biomes—such as boreal forest—an increase in temperature may translate into higher net primary production, more nutrients, and more biodiversity. The impact of climate change on these biomes is complex because the benefits may be minimized by the loss of

moisture through increased evapotranspiration. These findings are important by themselves, but it should be stressed that confidence in the previous results is contingent to model ability to correctly depict boundaries between climates. Climate models are powerful tools for environmental applications but have limitations and known uncertainties that should be taken into account in any discussion on those potential biome shifts.

Counterintuitively, we found that uncertainties derived from socio-economic scenarios are not critical for changes in biome distribution. Trends are similar for all SSPs but they differ in the intensity and the extent of the climate shifts. On the other hand, model uncertainties play a key role in future estimates, especially over regions with large inter-model variability. The lack of consensus for present climate affects the reliability of future projections of biomes and, consequently, the projected shifts should be carefully scrutinized, always having in mind that they are contingent upon how well the model represents precipitation in the first place. For ecotones, scenario and model uncertainties are equally important. Many climate shifts appear over regions with large model uncertainties. The western US, the Andes, the African Great Lakes, the Gobi Desert and the Tibetan Plateau are some but a few examples. The increase of spatial resolution can partially solve some problems—e.g. the wet bias in the Tibetan Plateau and Tropical Andes—but many errors inherent to the modeling are still present^{57,58}. Model limitations are often hidden to the environmental sciences community. Thus, for example, future biomes maps show a severe reduction of the Afrotropical Forest. If true, an adaptation plan would be urgent to minimize the potential loss of biodiversity⁵⁹. However, we know that those expected changes are subject to large uncertainties due to limitations in the modeling of precipitation. Discrepancies are clear in the consensus map but are buried in the MME mean. Similarly, inter-model variability impacts the future distribution of prairies in North America⁶⁰. The differences in precipitation percolate to biome classification and precludes a clear answer to expected changes. Forest tundra in the Tibetan Plateau is another climate hotspot that could lead to biome extinction if we trust the MME projections. We already know that the region is currently under high ecological risk due to rising temperatures⁶¹ but there is a lack of model consensus about how much territory will be affected because not only precipitation but also temperature uncertainties. Practitioners should put special focus on these

hidden errors in order to avoid potential pitfalls; otherwise that could lead to inappropriate policy decisions.

Some biases are intrinsically linked to the classification system. In Holdridge's scheme, life zones delineations have a logarithmic scale, which means that lower climate extremes (e.g. cold deserts) are more sensitive to small deviations in climate parameters. The incorrect classification of the Patagonian Desert by most models serves as a perfect example. The logarithmic scale can also affect higher climate extremes in a different way. Annual precipitation in tropical rainforest in Africa is between 1600 and 2000 mm yr⁻¹, slightly below the lower limit of this biome according to Holdridge's classification scheme. For that reason, CRU and models fail to correctly represent rainforests in Africa but they do in other rainier regions such as South America and the Maritime Continent (above >2000 mm yr⁻¹, on average). Although relevant, these types of errors are the easiest to be controlled through sensitivity analysis.

A potential source of uncertainty in biome and ecotone shifts is the way classification systems tackle potential evapotranspiration (PET). Holdridge's scheme is based on biotemperature, but other classifications include different variables such as wind speed, radiation and relative humidity⁶². Resulting differences in PET estimates are propagated to moisture conditions that define the boundaries of each life zone (PET ratio), introducing more uncertainty into predicted biome and ecotone shifts. A simple way to ensure predictions using PET are consistent with those not using it is to compare the outputs. Thus, if the models suffer from the same biases under different classifications, we can conclude that the uncertainties are unlikely to be due to PET misrepresentation. Similarly, if a region experiences a biome change under one type of classification, but not under the other, we can conclude that PET modeling may be playing a role⁶³.

In order to ascertain such potential uncertainty, we performed a comparison of Holdridge classification with Whittaker's biomes and Köppen's climate types. We found no significant difference. The affected areas by the shifts and their drivers (changes in precipitation) were similar for the three classification schemes, as are the regions affected by future biome shifts. This lends confidence to Holdridge's system ability to gauge biome and ecotone shifts in spite of not directly considering PET.

Future projections of terrestrial biomes are also affected by mismatches in source data. Fields with clear-cut gradients, such as precipitation, are difficult to measure even at highly aggregated levels. A major problem of gauge-based observations is that they have low spatial coverage and are generally undersampled in areas with complex orography. The montane forest between Mexican Sierras (Madre Oriental and Occidental) is the canonical example. We observed that CRU underestimates total annual precipitation and thus induces Holdridge to define the area as chaparral while most models classify it as a temperate forest, which is in agreement with in-situ observations of the green cover. This type of problem becomes critical when models are 'tuned' towards biased observations during the development stage, masking and propagating errors through the climate projections. Indeed, over-tuning may impact other variables than those tuned given the high non-linearity of the system^{64,65}.

Scale is another aspect that deserves attention. Model outputs are often combined with ecological and vegetation models for vulnerability assessments at a small spatial scale⁶⁶. However, precipitation estimates can only be adequately used using aggregated quantities and large domains, given the patchy nature and the large spatial variability of the field. Even at large temporal and spatial aggregations, errors exceeding 100% are common in precipitation estimates even for state-of-the-art climate models⁶⁷. The inherent uncertainty in the estimation of the input data is an important limitation for vulnerability models because downscaling amplifies the cascade of uncertainties in downstream models^{68,69}. Some biases in GCMs and ESMs are due

to known limitations in the parameterizations but many others are related to the still imperfect knowledge of the interactions between components of the climate system^{70,71}—so the 'inherent' label above. A standard way to cope with errors is by using bias correction methods, which are developed under the assumption that biases are constant over time. However, such statistical stationarity is a strong assumption not supported by empirical analyses. The suitability of that approach is even more unclear for future projections and several authors argued that its performance is highly dependent on the variable of interest, the area of study and the methodology^{72–74}.

Consensus maps of indicators such as biome and ecotone classes—e.g. Figure 2d—can be used to qualitatively pinpoint systematic errors in GCMs and ESMs. Another application of these maps is their use for monitoring biodiversity hotspots and its probability of risk, which is derived from the model consensus. An important assumption of our approach is that processes will operate in the same way in future climate giving that the physics will be the same—the *rosy scenario*—but that is strong assumption in the case of biogeographical variables. So far, and from the results shown here, we can only conclude that confident areas include: east North America and the Brazilian Cerrado; Most regions in Europe, including Fennoscandia; the Congo basin, and hot deserts in Africa and the Middle East; northern Russia and eastern China in Asia; the Maritime Continent and central northern regions of Australia.

In some other areas, however, and attending to a purely quantitative analysis (CRU, ground truth data for precipitation) there is less confidence in the use of GCMs and ESMs to gauge biodiversity shifts. Those include the west North America, Mesoamerica and the Caribbean South America, Tropical and Chilean Andes, and the Gran Chaco in America; eastern Afrotropical Forest in Africa; the Irano-Anatolian region, mountains of central Asia, and mountains of southwest China in Asia; and most of transitional zones. A major problem facing the community is that most of those areas are terrestrial hotspots of biodiversity.

In conclusion, despite the advances in recent years, climate models are far from being perfect and modeling water cycle remains the Achilles' heel of ESMs. The precise measurement of precipitation in the present climate is still challenging and affects biodiversity studies. In the case of future, estimates of precipitation are even more uncertain. An inadequate use of precipitation data in environmental models, one beyond the known limitations of precipitation measurement and modeling, may affect the conclusions of vulnerability assessment studies⁷⁵. Even the sign and amplitude of the error are uncertain: it could be either an overestimation or an underestimation of the impacts on biota and human life.

It is worth noting that Holdridge's approach, like any other classification method, is just an indirect way of defining biome distribution, one based on the mean state of key climate variables. We assume that the boundaries defining the classes remain constant over time and we use them to predict future biome shifts. The real world, however, is much more complex and field studies are the ultimate standard to inform policy decisions⁷⁶.

Here we have focused on the model side in order to identify whose areas are beyond confidence given our state of the art in precipitation science and those where our current knowledge grants us robust conclusions. Indeed, that does not mean that impacts in areas lacking consensus are to be dismissed or model results questioned there. On the contrary, notwithstanding the many caveats that may apply, global climate models are essential for a better understanding of how Earth's system works. Their outputs provide an accurate estimation of the changes in future climate, but a more solid conceptual and process understanding of climate model biases is required to be used in climate change vulnerability assessments. The point of evaluating climate models

is not to criticize them or imply that they are unsuitable for environmental applications, but rather to identify areas that need improvement and direct resources to fulfill those gaps.

METHODS

We used data from the climate models participating in phase six of the Coupled Intercomparison Project (CMIP6). We applied a modified version of Holdridge's life zones system⁷⁷ (HLZ) to evaluate model and multi-model ensembles for present climate and future scenarios. Models were ranked using Cohen's kappa coefficient (a qualitative evaluation of classes) and the agreement with observed precipitation (a quantitative estimate). Specifically, we used the following materials and methods.

Data

We used fifty-two Global Climate Models (GCMs) from the Coupled Intercomparison Project Phase 6 (CMIP6, see supplementary table 1 for a list)⁷⁸ to generate Holdridge's life zones classification system for present (1980–2014) and future climates (2015–2100). Additionally, we included a multi-model ensemble mean of fifty-two members (MME) and five ensembles of top-ranked models (T05, T10, T15, T25 and T40, see supplementary table 1 for a complete list of models). The reference dataset was Climate Research Unit Time Series version 4.04 (CRU)⁷⁹. Future life zones and ecotones were evaluated under seven scenarios (SSP1-1.9, SSP1-2.6, SSP4-3.4, SSP2-4.5, SSP3-7.0, SSP4-6.0, SSP5-8.5). Both the GCMs and observational datasets were interpolated to a horizontal resolution of 1.0×1.0 using a bilinear remapping method. The analysis was for land-only, excluding Antarctica. Data from CMIP6 models were downloaded from the ESGF. Reference data was obtained from the CEDA website. Soil carbon stocks and nitrogen were computed for each HLZ using the SoilGrids 2.0 dataset⁸⁰.

Holdridge life zones

HLZs are defined by three climatic measurements: annual precipitation (mm year^{-1}), biotemperature ($^{\circ}\text{C}$) and PET ratio. Annual precipitation (APR) was calculated from monthly precipitation data. Mean annual biotemperature (MAB) was derived from monthly average temperature. Those months with mean temperature over 30.00°C and below 0.00°C were omitted, as in the original method. PET ratio (PER) was defined as the mean annual biotemperature multiplied by a constant value (58.93) and divided by annual precipitation⁸¹. We assigned a class to each grid cell by computing the minimum Euclidean distance between each pixel and the geometric centroids of life zones as defined in Sisneros⁸² (see Supplementary Table 2 for details). The resulting 33 classes were aggregated into 13 major biomes following Monserud & Leemans⁸³. Maps of HLZs for individual models can be found in supplementary figures (Present: 1; Future: 8–14). Maps of MAB (Present: 4; Future: 30–36), APR (Present: 5; Future: 37–43), and PER (Present: 6; Future: 44–50) for present and future climates are also included in supplementary figures.

Transitional life zones (Ecotones)

Holdridge's classification system is a set of 36 hexagons in a triangular frame. Biotemperature, precipitation and PET ratio mark out six separated triangles in each hexagon which represent the ecotones (Fig. 1a). Each triangle connects 3 adjacent core zones (inner hexagons). For example, the three lines of precipitation (250 mm), biotemperature (3°C) and PET ratio (1.0) intersect to form triangle 5 (CP-FT-BF ecotone). As did for HLZs, we aggregated the initial 216 transitional life zones into 27 different classes. Supplementary table 3 includes a complete list of ecotones and their defining criteria. Maps and stem plots for

individual models can be found in Supplementary Figures (Present: 3, 51; Future: 22–28, 52–58).

Whittaker's biomes and Köppen's climate types

We complemented the analysis with two other classification schemes to ensure that the results were not linked to the chosen classification system. We used the modified version of Whittaker's biomes described in Ricklefs⁸⁴, which divides the Earth into nine biomes. Classification was performed using the R package *BIOMEplot*. For the Köppen scheme, we employed the standard algorithm as used in Navarro et al.⁸⁵. It classifies ecoregions into five distinct climate types, including one hydrologic type (B) and four thermal types (A, C, D, E). The algorithm also includes three subtypes (f, s, w) to capture the annual precipitation cycle.

Model rank

We used Cohen's kappa coefficient⁸⁶ to quantify the ability of individual models to reproduce Holdridge's life zones as depicted by CRU for the historical period (1980–2014). The kappa coefficient (κ) is defined as: $\kappa = \frac{P_0 - P_e}{1 - P_e}$, Where P_0 is the proportion of units with the agreement and P_e is the hypothetical probability of chance agreement. Grid boxes were weighted by area. The kappa statistic ranges from 0 (no agreement) to 1 (perfect agreement). Models are also ranked in terms of agreement with precipitation observations. The metric used was the coefficient of determination R^2 . We used Python packages *sklearn* v0.24.1 and *scipy* v1.6.1 to perform the statistical analysis. Individual scatter plots of annual precipitation can be found in Supplementary Fig. 7.

Qualitative methods for deconstructing errors and future changes in HLZs

We made a pixel-by-pixel comparison of modeled and observed life zones. If they were coincident, we codified those areas as "agreement". For mismatching areas, we computed the difference between the nearest geometric centroid for reference and modeled datasets for PET ratio, biotemperature and annual precipitation. Positive values indicate that reference data has higher values than model while negative values are otherwise. Zero means both are equal. Then, we applied the following algorithm:

The same procedure was done for future changes but comparing modeled life zones for present and future climate scenarios. Maps and donut plots of differences (changes) for individual models can be found in Supplementary Figures (Present: 2, 59; Future: 15–21, 60–66).

Mapping consensus

We compared the distribution of HLZs from top ten models (see Fig 1b for ranking models). Consensus was obtained when, at least, eight models agreed with reference data in the type of life zone. Dissent was defined when less than three models agreed with reference data. We classified as N/C those cases where models have moderate consensus (3–7 models). All computations are based on pixel-by-pixel comparison. The same procedure was performed for Whittaker's and Köppen's climate schemes.

Carbon and nitrogen stocks in the topsoil

We used SoilGrids 2.0 dataset to compute carbon and nitrogen in the topsoil (30 cm) for each pixel. Finally, we grouped all pixels that fall into each hexagon of Holdridge's scheme and then computed the average to obtain the resulting values for each hexagon.

DATA AVAILABILITY

CMIP6 model data sets used in this study are publicly available at <https://esgf-node.llnl.gov/search/cmip6/>. The CRU-TS gridded dataset can be found at <https://catalogue.ceda.ac.uk>. Gridded data on soil carbon/nitrogen was obtained from SoilGrids 2.0 and it can be found at <https://soilgrids.org>.

CODE AVAILABILITY

The codes used for all the analyses and visualization are available upon reasonable request to the corresponding author.

Received: 6 September 2023; Accepted: 19 January 2024;

Published online: 02 February 2024

REFERENCES

- Barlow, J. et al. Anthropogenic disturbance in tropical forests can double biodiversity loss from deforestation. *Nature* **535**, 144–147 (2016).
- Mantyka-Pringle, C. S. et al. Climate change modifies risk of global biodiversity loss due to land-cover change. *Biol. Conserv.* **187**, 103–111 (2015).
- Li, D., Wu, S., Liu, L., Zhang, Y. & Li, S. Vulnerability of the global terrestrial ecosystems to climate change. *Glob. Change Biol.* **24**, 4095–4106 (2018).
- Hochstrasser, T., Kröel-Dulay, G. Y., Peters, D. P. C. & Gosz, J. R. Vegetation and climate characteristics of arid and semi-arid grasslands in North America and their biome transition zone. *J. Arid Environ.* **51**, 55–78 (2002).
- Risser, P. G. The status of the science examining ecotones: a dynamic aspect of landscape is the area of steep gradients between more homogeneous vegetation associations. *BioScience* **45**, 318–325 (1995).
- Smith, A. J. & Goetz, E. M. Climate change drives increased directional movement of landscape ecotones. *Landsc. Change* **36**, 3105–3116 (2021).
- Fortin, M. J. et al. Issues related to the detection of boundaries. *Landsc. Ecol.* **15**, 453–466 (2000).
- Neilson, R. P. Transient ecotone response to climatic change: some conceptual and modelling approaches. *Ecol. Appl.* **3**, 385–395 (1993).
- Goldblum, D. & Rigg, L. S. The Deciduous Forest–Boreal Forest Ecotone. *Geogr. Compass* **4**, 701–717 (2010).
- Willis, K. J. & Whittaker, R. J. Species diversity-scale matters. *Science* **295**, 1245–1248 (2002).
- Holdridge, L. R. *Life Zone Ecology* (Tropical Science Center, 1967).
- Lugo, A. E., Brown, S. L., Dodson, R., Smith, T. S. & Shugart, H. H. The Holdridge life zones of the conterminous United States in relation to ecosystem mapping. *J. Biogeogr.* **26**, 1025–1038 (1999).
- Cañadas, L. & Estrada, W. The Effects on Holdridge Life zones, in *The Impact of Climatic Variations on Agriculture: Volume 2: Assessments in Semi-Arid Regions* (eds Parry, M.L. et al.) 473–484 (Springer, 1988).
- Box, E. O. & Fujiiwara, K. in *Vegetation Ecology* 455–485 (John Wiley & Sons, 2013).
- Jiang, M., Felzer, B. S., Nielsen, U. N. & Medlyn, B. E. Biome-specific climatic space defined by temperature and precipitation predictability. *Glob. Ecol. Biogeogr.* **26**, 1270–1282 (2017).
- Woodward, F. I., Lomas, M. R. & Kelly, C. K. Global climate and the distribution of plant biomes. *Philos. Trans. R. Soc. B* **359**, 1465–1476 (2004).
- Lin, Y.-S. et al. Optimal stomatal behaviour around the world. *Nat. Clim. Change* **5**, 459–464 (2015).
- Moles, A. T. et al. Which is a better predictor of plant traits: temperature or precipitation? *J. Veg. Sci.* **25**, 1167–1180 (2014).
- Stephens, R. E. et al. Climate shapes community flowering periods across biomes. *J. Biogeogr.* **49**, 1205–1218 (2022).
- Fan, Z.-M., Li, J. & Yue, T.-X. Land-cover changes of biome transition zones in Loess Plateau of China. *Ecol. I Model.* **252**, 129–140 (2013).
- Szelepčsényi, Z., Breuer, H. & Sümegei, P. The climate of Carpathian Region in the 20th century based on the original and modified Holdridge life zone system. *Centr Eur. J. Geosci.* **6**, 293–307 (2014).
- Flato, G. M. Earth system models: an overview. *WIREs Clim. Change* **2**, 783–800 (2011).
- Schoeman, D. S. et al. Demystifying global climate models for use in the life sciences. *Trends Ecol. Evol.* **38**, 843–858 (2023).
- Bayar, A. S., Yilmaz, M. T., Yücel, I. & Dirmeyer, P. CMIP6 earth system models project greater acceleration of climate zone due to stronger warming rates. *Earth's Future* **11**, e2022EF002972 (2023).
- Evans, P. & Brown, C. D. The boreal–temperate forest ecotone response to climate change. *Environ. Rev.* **25**, 423–431 (2017).
- Noble, I. R. A model of the responses of ecotones to climate change. *Ecol. Appl.* **3**, 396–403 (1993).
- Wasson, K., Woolfolk, A. & Fresquez, C. Ecotones as indicators of changing environmental conditions: rapid migration of salt marsh-upland boundaries. *Estuaries. Coast* **36**, 654–664 (2013).
- Stouffer, R. J. et al. CMIP5 Scientific Gaps and Recommendations for CMIP6. *Bull. Am. Meteorol. Soc.* **98**, 95–105 (2017).
- Mueller, B. & Seneviratne, S. I. Systematic land climate and evapotranspiration biases in CMIP5 simulations. *Geophys. Res. Lett.* **41**, 128–134 (2014).
- Lin, Y. et al. Causes of model dry and warm bias over central U.S. and impact on climate projections. *Nat. Commun.* **8**, 881 (2017).
- Ma, H.-Y., Zhang, K., Tang, S., Xie, S. & Fu, R. Evaluation of the causes of wet-season dry biases over Amazonia in CAM5. *J. Geophys. Res. Atmos.* **126**, e2020JD033859 (2021).
- Hagos, S. M. et al. The relationship between precipitation and precipitable water in CMIP6 simulations and implications for tropical climatology and change. *J. I Clim.* **34**, 1587–1600 (2021).
- Sun, C. & Liang, X.-Z. Understanding and reducing warm and dry summer biases in the Central United States: analytical modeling to identify the mechanisms for CMIP ensemble error spread. *J. Clim.* **36**, 2035–2054 (2023).
- Booth, T. H. Checking bioclimatic variables that combine temperature and precipitation data before their use in species distribution models. *Aust. Ecol.* **47**, 1506–1514 (2022).
- Harris, R. M. B. et al. Climate projections for ecologists. *WIREs Clim. Change* **5**, 621–637 (2014).
- Dai, A., Zhao, T. & Chen, J. Climate change and drought: a precipitation and evaporation perspective. *Curr. Clim. Change Rep.* **4**, 301–312 (2018).
- Grose, M. R. et al. Insights from CMIP6 for Australia's future climate. *Earth's Future* **8**, e2019EF001469 (2020).
- Yin, L., Fu, R., Shevliakova, E. & Dickinson, R. E. How well can CMIP5 simulate precipitation and its controlling processes over tropical South America? *Clim. Dyn.* **41**, 3127–3143 (2013).
- Almazroui, M. et al. Projected changes in temperature and precipitation over the United States, Central America, and the Caribbean in CMIP6 GCMs. *Earth Syst. Environ.* **5**, 1–24 (2021).
- Ryu, J.-H. & Hayhoe, K. Understanding the sources of Caribbean precipitation biases in CMIP3 and CMIP5 simulations. *Clim. Dyn.* **42**, 3233–3252 (2014).
- Sengupta, A. et al. Representation of atmospheric water budget and uncertainty quantification of future changes in CMIP6 for the Seven U.S. National Climate Assessment Regions. *J. Clim.* **35**, 7235–7258 (2022).
- Fiedler, S. et al. Simulated tropical precipitation assessed across three major phases of the Coupled Model Intercomparison Project (CMIP). *Mon. Weather Rev.* **148**, 3653–3680 (2020).
- Liu, Z., Mehran, A., Phillips, T. J. & AghaKouchak, A. Seasonal and regional biases in CMIP5 precipitation simulations. *Clim. Res.* **60**, 35–50 (2014).
- Houze, R. A. Orographic effects on precipitating clouds. *Rev. Geophys.* **50**, RG1001 (2012).
- O'Neill, B. C. et al. A new scenario framework for climate change research: the concept of shared socioeconomic pathways. *Clim. Change* **122**, 387–400 (2014).
- Lawrence, D., Coe, M., Walker, W., Verchot, L. & Vandecar, K. The unseen effects of deforestation: biophysical effects on climate. *Front. Glob. Change* **5**, 756115 (2022).
- Maaroufi, N. I. & De Long, J. R. Global change impacts on forest soils: linkage between soil biota and carbon-nitrogen-phosphorus stoichiometry. *Front. Glob. Change* **3**, 16 (2020).
- Walther, G.-R. et al. Alien species in a warmer world: risks and opportunities. *Trends Ecol. Evol.* **24**, 686–693 (2009).
- Lee, X. et al. Observed increase in local cooling effect of deforestation at higher latitudes. *Nature* **479**, 384–387 (2011).
- Jungkunst, H. F., Goepel, J., Horvath, T., Ott, S. & Brunn, M. New uses for old tools: reviving Holdridge Life Zones in soil carbon persistence research. *J. Plant Nutr. Soil Sci.* **184**, 5–11 (2021).
- Post, W. M., Pastor, J., Zinke, P. J. & Stangenberger, A. G. Global patterns of soil nitrogen storage. *Nature* **317**, 613–616 (1985).
- Dexter, K. G. et al. Inserting tropical dry forests into the discussion on biome transitions in the tropics. *Front. Ecol. Evol.* **6**, 104 (2018).
- Siyum, Z. G. Tropical dry forest dynamics in the context of climate change: syntheses of drivers, gaps, and management perspectives. *Ecol. Process.* **9**, 25 (2020).
- Murphy, P. G. & Lugo, A. E. Ecology of tropical dry forest. *Annu. Rev. Ecol. Syst.* **17**, 67–88 (1986).
- Toby Pennington, R., Prado, D. E. & Pendry, C. A. Neotropical seasonally dry forests and Quaternary vegetation changes. *J. Biogeogr.* **27**, 261–273 (2000).
- Snyder, K. A. et al. Effects of changing climate on the hydrological cycle in cold desert ecosystems of the Great Basin and Columbia Plateau. *Rangel. Ecol. Manag.* **72**, 1–12 (2018).

57. Chen, Q., Ge, F., Jin, Z. & Lin, Z. How well do the CMIP6 HighResMIP models simulate precipitation over the Tibetan Plateau? *Atmos. Res.* **279**, 106393 (2022).
58. Monerie, P. A., Chevuturi, A., Cook, P., Klingaman, N. P. & Holloway, C. E. Role of atmospheric horizontal resolution in simulating tropical and subtropical South American precipitation in HadGEM3-GC31. *Geosci. Model Dev.* **13**, 4749–4771 (2020).
59. Martens, C. et al. Large uncertainties in future biome changes in Africa call for flexible climate adaptation strategies. *Glob. Change Biol.* **27**, 340–358 (2021).
60. Barrow, E. M. & Sauchyn, D. J. Uncertainty in climate projections and time of emergence of climate signals in the western Canadian Prairies. *Int. J. Clim.* **39**, 4358–4371 (2019).
61. Wang, S., Liu, F., Zhou, Q., Chen, Q. & Liu, F. Simulation and estimation of future ecological risk on the Qinghai-Tibet Plateau. *Sci. Rep.* **11**, 17603 (2021).
62. Zomer, R. J., Xu, J. & Trabucco, A. Version 3 of the Global Aridity Index and Potential Evapotranspiration Database. *Sci. Data* **9**, 409 (2022).
63. Scheiter, S., Kumar, D., Pfeiffer, M. & Langan, L. Biome classification influences current and projected future biome distributions. *Glob. Ecol. Biogeogr.* **33**, 1–13 (2023).
64. Hourdin, F. et al. The art and science of climate model tuning. *Bull. Am. Meteorol. Soc.* **98**, 589–602 (2017).
65. Schneider, T., Lan, S., Stuart, A. & Teixeira, J. Earth system modeling 2.0: a blueprint for models that learn from observations and targeted high-resolution simulations. *Geophys. Res. Lett.* **44**, 396–12,417 (2017).
66. Dawson, T. P., Jackson, S. T., House, J. I., Prentice, I. C. & Mace, G. M. Beyond predictions: biodiversity conservation in a changing climate. *Science* **332**, 53–58 (2011).
67. Tapiador, F. J. et al. Is precipitation a good metric for model performance? *Bull. Am. Meteorol. Soc.* **100**, 223–233 (2019).
68. Ahlström, A., Schurgers, G. & Smith, B. The large influence of climate model bias on terrestrial carbon cycle simulations. *Environ. Res. Lett.* **12**, 014004 (2017).
69. Wu, Z. et al. Climate data induced uncertainty in model-based estimations of terrestrial primary productivity. *Environ. Res. Lett.* **12**, 064013 (2017).
70. Betz, G. Are climate models credible worlds? Prospects and limitations of probabilistic climate prediction. *Eur. J. Philos. Sci.* **5**, 191–215 (2015).
71. Neumann, P. et al. Assessing the scales in numerical weather and climate predictions: will exascale be the rescue? *Philos. Trans. R. Soc. A* **377**, 20180148 (2019).
72. Chen, J., Brissette, F. P. & Caya, D. Remaining error sources in bias-corrected climate model outputs. *Clim. Change* **162**, 563–582 (2020).
73. Manzanos, R., Lucero, A., Weisheimer, A. & Gutiérrez, J. M. Can bias correction and statistical downscaling methods improve the skill of seasonal precipitation forecasts? *Clim. Dyn.* **50**, 1161–1176 (2018).
74. Maraun, D. et al. Towards process-informed bias correction of climate change simulations. *Nat. Clim. Change* **7**, 764–773 (2017).
75. Slingo, J. et al. Ambitious partnership needed for reliable climate prediction. *Nat. Clim. Change* **12**, 499–503 (2022).
76. Lian, X. et al. Multifaceted characteristics of dryland aridity changes in a warming world. *Nat. Rev. Earth Environ.* **2**, 232–250 (2021).
77. Holdridge, L. R. Determination of world plant formations from simple climatic data. *Science* **105**, 367–368 (1947).
78. Eyring, V. et al. Overview of the Coupled Model Intercomparison Project Phase 6 (CMIP6) experimental design and organization. *Geosci. Model Dev.* **9**, 1937–1958 (2016).
79. Harris, I., Jones, P. D. D., Osborn, T. J. J. & Lister, D. H. H. Updated high-resolution grids of monthly climatic observations—the CRU TS3.10 Dataset. *Int. J. Clim.* **34**, 623–642 (2014).
80. Poggio, L. et al. SoilGrids 2.0: producing soil information for the globe with quantified spatial uncertainty. *SOIL* **7**, 217–240 (2021).
81. Holdridge, L. R. Simple method for determining potential evapotranspiration from temperature data. *Science* **130**, 572–572 (1959).
82. Sisneros, R., Huang, J., Ostrouchov, G. & Hoffman, F. Visualizing life zone boundary sensitivities across climate models and temporal spans. *Procedia Comput. Sci.* **4**, 1582–1591 (2011).
83. Monserud, R. A. & Leemans, R. Comparing global vegetation maps with the Kappa statistic. *Ecol. Model.* **62**, 275–293 (1992).
84. Ricklefs, R. E. *The Economy of Nature* 6th edn (W.H. Freeman and Co., (2008).
85. Navarro, A. et al. Towards better characterization of global warming impacts in the environment through climate classifications with improved global models. *Int. J. Climatol.* **42**, 5197–5217 (2022).
86. Cohen, J. A coefficient of agreement for nominal scales. *Educ. Psychol. Meas.* **20**, 37–46 (1960).

ACKNOWLEDGEMENTS

A.N. acknowledges funding from the Regional Government of Castilla-La Mancha (SBPLY/22/180502/000019). F.J.T. acknowledges funding from the Spanish Ministry of Science (PID2022-138298OB-C22, PDC2022-133834-C21, TED2021-131526B-I00). R.M. acknowledges funding from the Spanish Ministry of Science (PID2020-113443RB-C21, TED2021-131526B-I00). This work was funded by the Korea Meteorological Administration Research and Development Program under Grant RS-2023-00237740.

AUTHOR CONTRIBUTIONS

A.N.: conceptualization, formal analysis, investigation, methodology, visualization, writing, review & editing, funding acquisition. G.L.: formal analysis, visualization, writing. R.M.: formal analysis, methodology, writing. F.J.T.: formal analysis, investigation, writing, review & editing, funding acquisition, supervision. All authors substantially contributed to the article and approved the final manuscript.

COMPETING INTERESTS

The authors declare no competing interests.

ADDITIONAL INFORMATION

Supplementary information The online version contains supplementary material available at <https://doi.org/10.1038/s41612-024-00581-w>.

Correspondence and requests for materials should be addressed to Andrés. Navarro.

Reprints and permission information is available at <http://www.nature.com/reprints>

Publisher's note Springer Nature remains neutral with regard to jurisdictional claims in published maps and institutional affiliations.



Open Access This article is licensed under a Creative Commons Attribution 4.0 International License, which permits use, sharing, adaptation, distribution and reproduction in any medium or format, as long as you give appropriate credit to the original author(s) and the source, provide a link to the Creative Commons license, and indicate if changes were made. The images or other third party material in this article are included in the article's Creative Commons license, unless indicated otherwise in a credit line to the material. If material is not included in the article's Creative Commons license and your intended use is not permitted by statutory regulation or exceeds the permitted use, you will need to obtain permission directly from the copyright holder. To view a copy of this license, visit <http://creativecommons.org/licenses/by/4.0/>.

© The Author(s) 2024